Color normalization for robust evaluation of microscopy images

Jan Švihlík[a,c], Jan Kybic[a], David Habart[b]

[a] Czech Technical University in Prague, Technická 2, Prague, Czech Republic
[b] Institute for Clinical and Experimental Medicine, Vídeňská 1958/9, Prague, Czech Republic
[c] University of Chemistry and Technology, Technická 5, Prague, Czech Republic

ABSTRACT

This paper deals with color normalization of microscopy images of Langerhans islets in order to increase robustness of the islet segmentation to illumination changes. The main application is automatic quantitative evaluation of the islet parameters, useful for determining the feasibility of islet transplantation in diabetes. First, background illumination inhomogeneity is compensated and a preliminary foreground/background segmentation is performed. The color normalization itself is done in either $l\alpha\beta$ or logarithmic RGB color spaces, by comparison with a reference image. The color-normalized images are segmented using color-based features and pixel-wise logistic regression, trained on manually labeled images. Finally, relevant statistics such as the total islet area are evaluated in order to determine the success likelihood of the transplantation.

The robustness of the evaluation is increased dramatically by the color normalization, decreasing the image-wise failure rate from 17 % to 0 % and the equal error rate from 30 % to 1 %.

Keywords: S egmentation, color normalization, Langerhans islets, microscopy images

1. INTRODUCTION

Transplantation of isolated pancreatic islets from cadaver donors is a promising therapy for patients with the type 1 diabetes.[1] To determine the quality of isolated islets and their suitability for successful transplantation, microscopy images of islet graft samples are acquired and the quantity and size of the islets is evaluated. See Figure 2.

The processing of islet samples was at very time consuming using manual islet counting and size measurement through the microscope with calibrated micrometer grid.,[2] which is very time consuming. Later on, semi-automated[3] and automated methods appeared[4–6] to increase the reproducibility and speed of the analysis. In most methods, the first step is the image segmentation to identify individual islets. Then, the area and/or dimensions of each islet are evaluated. In some cases, the islet 3D volumes are estimated from the 2D measurements.

The segmentation can be performed by thresholding[7] or active contours.[8] Our method[9] is based on RGB color channel features and a logistic regression classifier, trained on a set hand-labeled images. However, this method assumes the class color distributions to be known and constant, which is not the case for images acquired in typical clinical settings, where the imaging protocol is often not fully respected and hence the staining and illumination varies considerably.

The aim of this paper is to develop a segmentation algorithm robust against the illumination and staining variability using a color normalization approach.

The simple color transfer between two images can be found in,[10] where the color normalization is done globally for whole image. A more advanced approach was published in,[11] where the authors used k-means clustering to create a mask which identifies several image classes.

Further author information: (Send correspondence to J. Švihlík)
J. Švihlík: E-mail: jan.svihlik@fel.cvut.cz, Telephone: +420 224 357 590

2. METHOD

2.1 Normalization of nonuniform illumination

First, we compensate for the non-uniform spatial illumination intensity. The islets are approximately identified by thresholding, obtaining a preliminary image segmentation. This islet pixel mask can be morphological dilated with a disk element to expand the islet sizes, so that no islet pixel is considered as background. Then, the background, non-islet areas are fitted in the least squares sense by a second order polynomial to obtain a smooth background intensity model. An example of the recovered illumination profile can be seen in Fig. 1.

2.2 Global color normalization

The images are first converted into a $l\alpha\beta$[11] or logarithmic RGB color space. The logarithmic RGB color space[12] is given by $C_{log} = \log(C+1)$. In either case, the mean and standard deviations are calculated for both the source and reference images. The colors are then transformed linearly[10] so that the means and standard deviations agree:

$$C_n = \frac{\sigma_{ref}}{\sigma}(C - \bar{C}) + \bar{C}_{ref}, \tag{1}$$

where C denotes the input color vector, e.g. (l, α, β), and $\bar{C}$ its mean value; C_n denotes is the output color, $\bar{C}_{ref}$ and σ_{ref} denote the mean color value and its standard deviation in the reference image. Note that addition in the logarithmic space corresponds to multiplication in the direct (e.g. RGB) space, which conforms to the standard multiplicative image generation model.

2.3 Multiclass color normalization

As in our case the color transformation might be different from class to class due to differences in the staining procedure, we adopt the following approach, inspired by:[11]

1. K-means clustering in the transformed color space is used to estimate the islet and background classes. The class with the least area is assumed to correspond to islets. If other tissue is present in the sample or if the background is inhomogeneous, we recommend to increase the number of classes k. Non-foreground classes can be merged together for the purpose of further processing.

2. We use $k = 3$, where two of three classes (a, b and c) are merged together based on minimal Euclidean distance ($\mathcal{D}_{a,b}$, $\mathcal{D}_{b,c}$, $\mathcal{D}_{a,c}$) computed between centroids (T_a, T_b and T_c) of several classes. Each centroid have RGB or $l\alpha\beta$ coordinates.

3. Mathematical morphology operation with a disk structuring element is used to clean and expand the islet area, which otherwise tends to be undersegmented.

4. The mean and standard deviation is calculated for each class in both images. The class correspondences are found. The class with the least area is assumed to correspond to islets.

5. Finally, each class is color-normalized separately using equation (1).

3. RESULTS

There are 141 clinical images in our database acquired during the past years under different illumination conditions. We shall call them the B set. We use a classifier[9] trained on another set of 46 images (called A), where the ground truth segmentations are available, see Fig. 2. This original classifier fails on about 17% of images from the B set. We have therefore applied the color normalization described in Section 2 on the B images, using one randomly selected image from the A set as a reference. After the normalization all segmentations are correct using visual inspection. In order to evaluate the pixel-wise performace quantitatively, we created 10 ground truth pixel-level segmentations (fully-manual segmentation) for selected images from the B set, see Fig. 3.The ROC curve was constructed using the classifier trained on the 46 A images and tested on all pixels of the manually segmented images B. The comparison between no color normalization and color normalization using $l\alpha\beta$ and

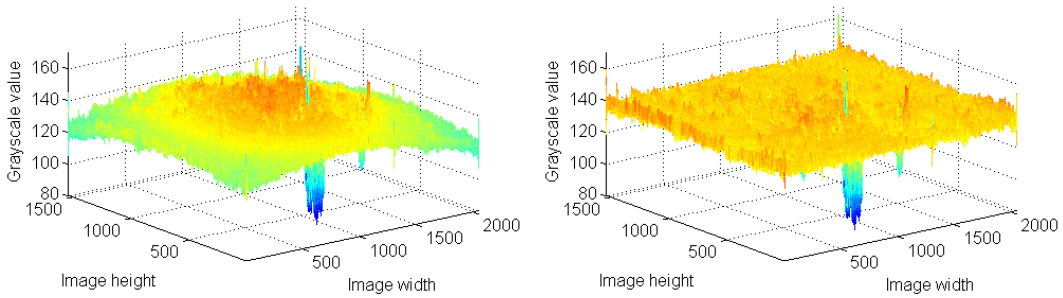

(a) R channel, unnormalized

(b) R channel, normalized non-uniform illumination

Figure 1. Example of normalization of non-uniform illumination.

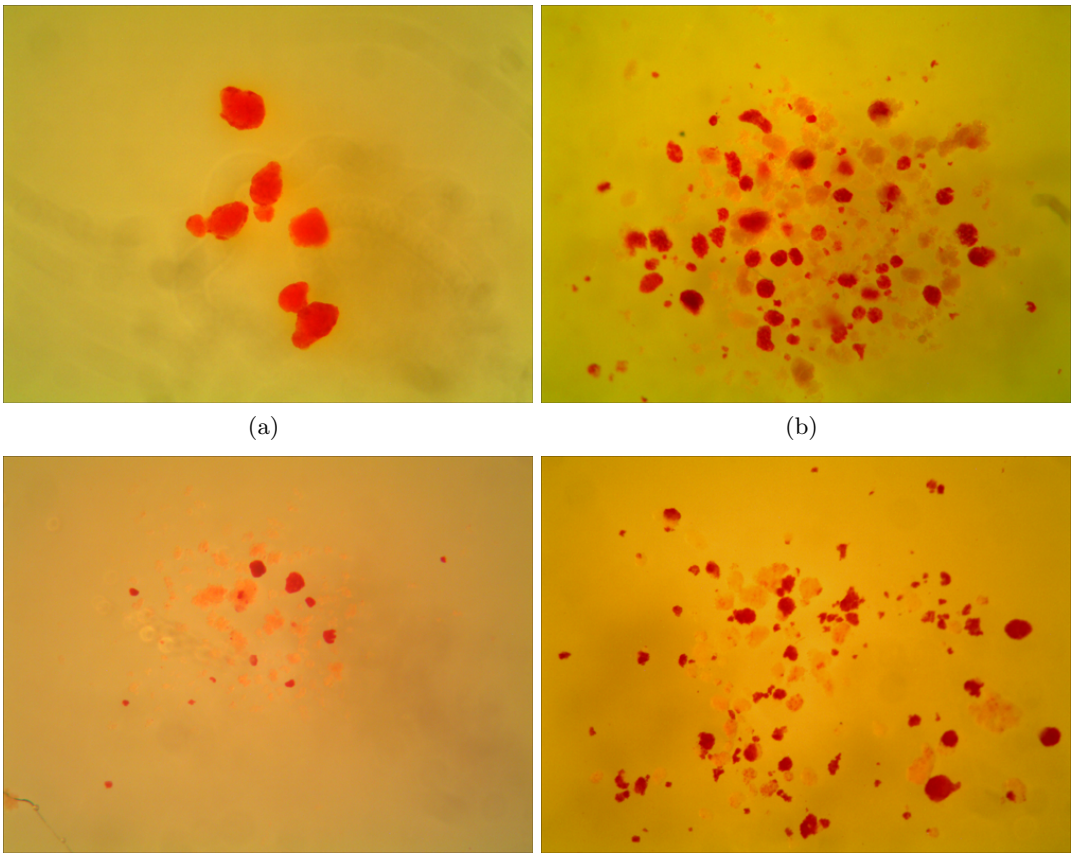

(a)

(b)

(c)

(d)

Figure 2. Example of images from the A set of 46 testing images consisting of four subsets. Every subset was taken under different light conditions.

logarithmic RGB color spaces can be seen in Fig. 4. We see that the equal error rate is improved from 30 % to 1 %.

We also evaluated mean sensitivity, mean precision and mean area ratio, see Tab. 1 The area ratio is defined as ratio between islet area detected at segmentation and islet area detected at ground truth segmentation. The evaluation of segmentation quality can be seen in Fig. 5. We tested clustering in the logarithmic RGB and $l\alpha\beta$ color space, with very similar results.

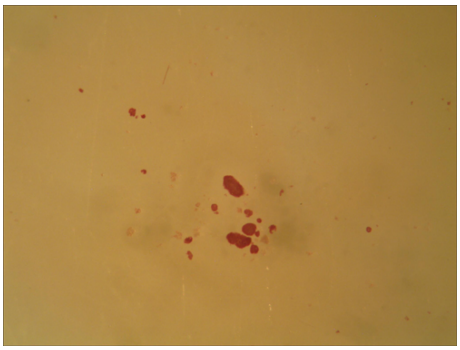

(a) small amount of exocrine tissue

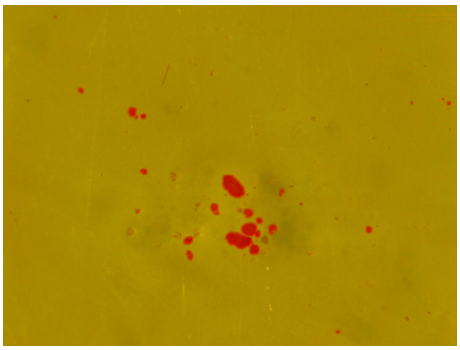

(b) normalized in $l\alpha\beta$ space

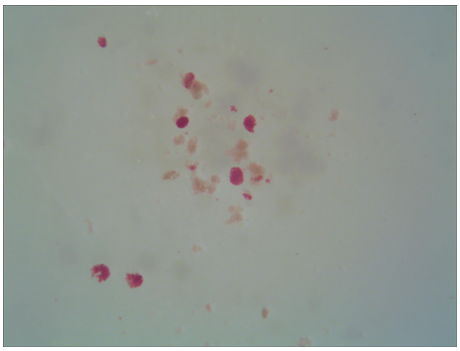

(c) more exocrine tissue

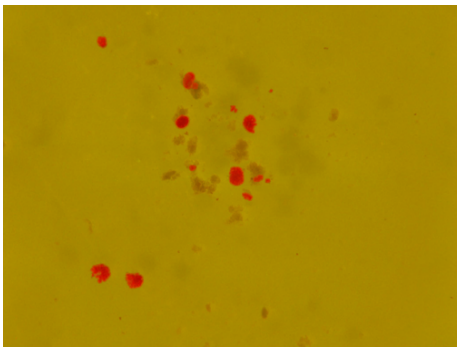

(d) normalized in $l\alpha\beta$ space

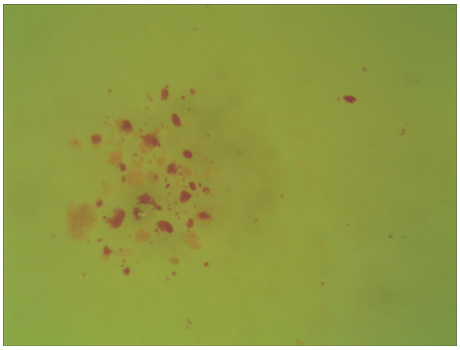

(e) embedded islets

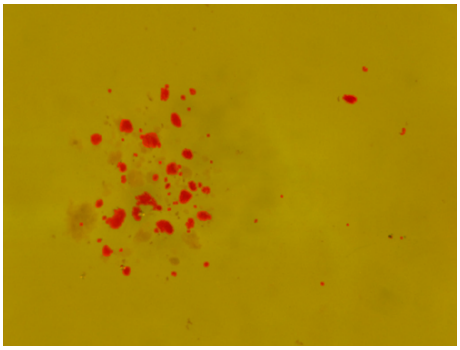

(f) normalized in $l\alpha\beta$ space

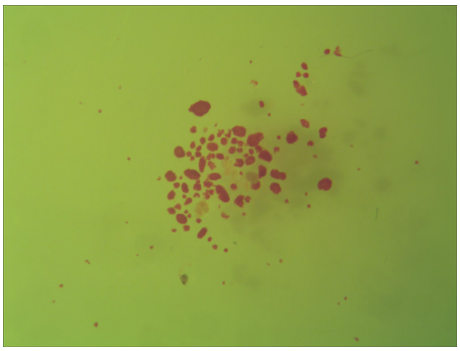

(g) small amount of exocrine tissue

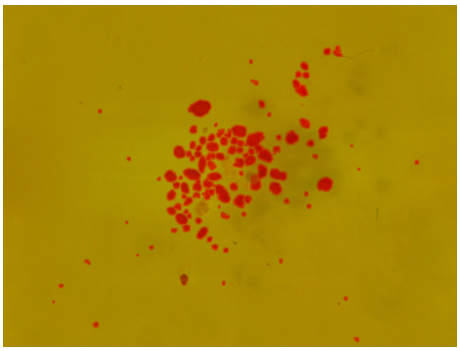

(h) normalized in $l\alpha\beta$ space

Figure 3. Left: unnormalized images from B set, Right: normalized in $l\alpha\beta$ space.

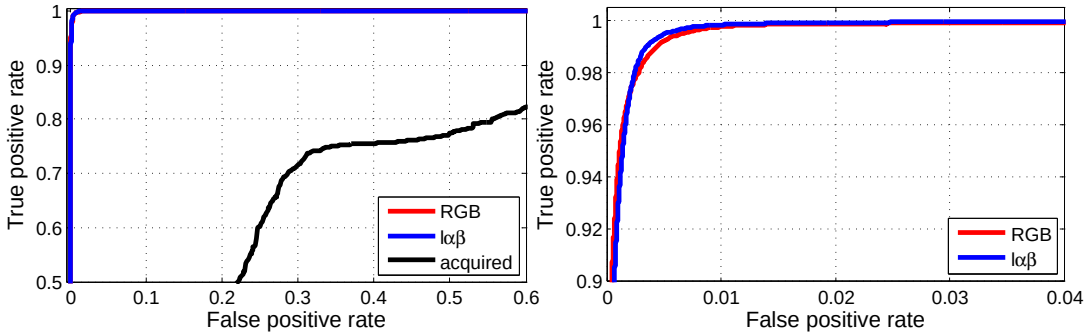

(a) (b)

Figure 4. (a) ROC curve computed for unnormalized data (black), data normalized in color (RGB space) and data normalized in color ($l\alpha\beta$ space), (b) detail of ROC curve for data normalized in color in RGB and $l\alpha\beta$.

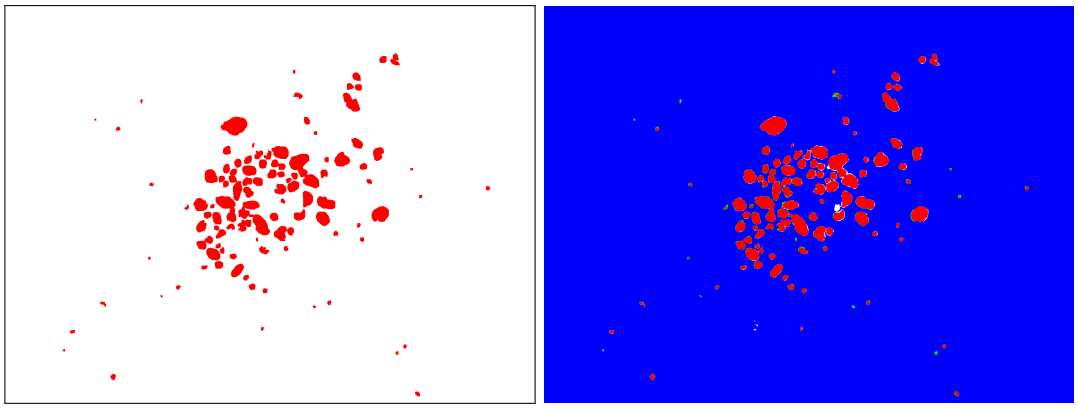

(a) unnormalized image (b) color-normalized

Figure 5. Comparison of segmentation with ground truth segmentation (a) unnormalized image, (b) color-normalized, True Positive (RED), True Negative (BLUE), False Positive (WHITE), False Negative (GREEN).

RGB	*sensitivity*	*precision*	*area ratio*
mean	0.9297	0.8591	1.0931
SD	0.0501	0.0814	0.1360

lαβ	*sensitivity*	*precision*	*area ratio*
mean	0.9251	0.8769	1.0622
SD	0.0464	0.0666	0.1149

Table 1. Statistical measures of segmented images normalized in color in both color spaces and ground truth segmentations. The area ratio is defined as ratio between islet area detected at segmentation and islet area detected at ground truth segmentation

4. CONCLUSION

In this paper we presented method for color normalization of microscopy images of Langerhans islets. For the selected images from our database of 141 clinical images we created fully manual segmentations which serve as the ground truth. We tested normalization in two color spaces, logarithmic RGB and $l\alpha\beta$. The computed ROC curves showed that the better results were given by color normalization in $l\alpha\beta$ space.

ACKNOWLEDGMENTS

This work has been supported by the grant 14-10440S "Automatic analysis of microscopy images of Langerhans islets" of the Czech Science Foundation.

REFERENCES

[1] R. Alejandro, F. B. Barton, B. J. Hering, S. Wease, and C. I. T. R. Investigators, "Update from the collaborative islet transplant registry," *Transplantation* **86**(12), pp. 1783–1788, 2008.

[2] C. Ricordi, D. W. Gray, B. J. Hering, and et al., "Islet isolation assessment in man and large animals," *Acta Diabetologica Latina* **27**(3), pp. 185–195, 1990.

[3] P. Girman, J. Kriz, and F. Saudek, "Digital imaging as a possible approach in evaluation of islet yield. cell transplantation," *Transplantation* **12**(2), pp. 129–133, 2003.

[4] K. J. Wile, T. J. Fetterhoff, D. Coffing, T. J. Cavanagh, and M. J. Wright, "Morphologic analysis of pancreatic islets automated image analysis," *Transplantation Proceedings* **26**(6), p. 3441, 1994.

[5] A. S. Friberg, "Quantification of the islet product: Presentation of a standardized current good manufacturing practices compliant system with minimal variability," *Transplantation* **91**(6), pp. 677–683, 2011.

[6] L. M. Rato, F. Capela e Silva, A. R. Costa, and et al., "Analysis of pancreas histological images for glucose intolerance identification using imagej-preliminary results," in *Proc. 4th Eccomas Thematic Conference on Computational Vision and Medical Image Processing (VipIMAGE)*, pp. 319–322, SPIE, 2014.

[7] J. P. Stegemann, J. J. O'Neil, D. T. Nicholson, and C. J. Mullon, "Improved assessment of isolated islet tissue volume using digital image analysis," *Cell Transplantation* **7**(5), pp. 469–478, 1998.

[8] C. Berclaz, J. Goulley, M. Villinger, and et al, "Diabetes imagingquantitative assessment of islets of langerhans distribution in murine pancreas using extended-focus optical coherence microscopy," *Biomedical Optics Express* **3**(6), pp. 1365–1380, 2012.

[9] J. Švihlík, J. Kybic, D. Habart, Z. Berková, P. Girman, J. Kříž, and K. Zacharovová, "Classification of microscopy images of langerhans islets," in *Medical Imaging 2014: Image Processing*, **9034**, pp. 1–8, SPIE, SPIE, (Bellingham, USA), March 2014.

[10] E. Reinhard, N. Ashikhmin, B. Gooch, and P. Shirley, "Color transfer between images," *IEEE Computer Graphics and Applications* **21**, pp. 34–41, September 2001.

[11] C. Mosquer-Lopez and S. Agaian, "Iterative local color normalization using fuzzy image clustering," in *Proc. SPIE 8755, Mobile Multimedia/Image Processing, Security, and Applications 2013*, **8755**, pp. 8755–1–8755–12, SPIE, 2013.

[12] G. Finlayson and R. Xu, "Illuminant and gamma comprehensive normalisation in log rgb space," *Pattern Recognition Letter* **24**(11), pp. 1679–1690, 2003.